

Atomic force microscope images of lipid layers spread from vesicle suspensions

Inger Vikholm ^{a,*}, Jouko Peltonen ^b, Olle Teleman ^c

^a Chemical Technology, Technical Research Centre of Finland, P.O. Box 14021, FIN-33101 Tampere, Finland

^b Department of Physical Chemistry, Åbo Akademi University, Turku, Finland

^c Biotechnology and Food Research, Technical Research Centre of Finland, Espoo, Finland

Received 26 May 1994; revised 2 September 1994; accepted 21 September 1994

Abstract

The layer formation of unilamellar vesicles of L- α -dimyristoyl phosphatidylcholine (DMPC) spread onto the air/liquid interface has been investigated. The layers were transferred to clean glass slides and onto slides made hydrophobic with multilayers of Cd arachidate. Aged vesicle suspensions aggregate during storage and are transferred as large domains as imaged with atomic force microscopy (AFM). Freshly prepared vesicles fuse and can be transferred as monolayers to hydrophobic supports. Furthermore, AFM images reveal the importance of positioning the solid support parallel to the moving barrier in order to obtain more uniform deposition of Cd arachidate.

Keywords: Vesicle fusion; Lipid layer; Langmuir-Blodgett film; Protein immobilization; Atomic force microscopy; Quartz crystal microbalance

1. Introduction

The incorporation of proteins into phospholipid layers has received considerable interest due to the application of these films in biosensors. Neither of the most commonly used techniques for enzyme immobilization – physical adsorption, entrapment, cross-linking or covalent bonding is, however, able to achieve a monolayer of receptor molecules reliably coupled to a solid support [1,2]. An alternative way to produce artificial membranes is to make layers by spreading from vesicles. Vesicles can be regarded as the simplest closed membrane model, resembling the natural surrounding of biomolecules. Biomolecules can easily be incorporated into vesicles. Bilayers can be prepared by allowing small unilamellar vesicles to come into contact with a solid support [3–7]. The adhesion and fusion of vesicles onto solid supports are, however, dependent on the size of the liposomes, lipid composition, flow rate, pH, and salt concentration [7–9]. Fusion of vesicles with cell membranes has received extensive interest as they can deliver concentrated doses of medication to diseased tissues [10]. Unilamellar vesicles

have also been reported to fuse and form monolayers at the air/liquid interface [11–14]. Proteins have been incorporated into these films, but the fusion is a complex process and still not fully understood. Fare et al. [15] obtained a non-uniform film consisting of domains of a lipid monolayer and protein-lipid multilayers, along with incompletely fused vesicles, when transferring the film onto a solid support.

Aldose dehydrogenase (ALDH) from *Gluconobacter oxydans* is a membrane-bound protein, that could be used as a biological component in an amperometric biosensor [16]. ALDH can not be isolated from the lipid environment without denaturation and was therefore embedded in vesicles to ensure that the protein was kept in its natural lipid environment. Our primary goal was to study the layer formation of both pure and ALDH containing L- α -dimyristoylphosphatidylcholine (DMPC) vesicles spread onto an air/liquid interface. The layers were transferred onto clean glass slides and slides coated with multilayers of Cd arachidate. The mass of the transferred layers was measured with a quartz crystal microbalance (QCM). Atomic force microscopy (AFM) was used to obtain detailed topographical information about the layers. AFM has rapidly become an illustrative tool commonly used in surface characterization. AFM can be used to image structural packing features of LB-films at molecular resolution and has also recently been used to image proteins [15,17–22].

* Corresponding author. E-mail: inger.vikholm@vtt.fi. Fax: +358 31 3163319.

Langmuir-Blodgett (LB) films are often used as supports for lipid layers and care should be taken to obtain perfect layers. The homogeneity depends not only on the monolayer material, but on a variety of factors such as ions in the subphase, pH, surface pressure, ageing, support, transfer rate and transfer mode [23–29]. Controversial results about the proper transfer mode have been presented [28–30], but normally the transfer mode used during deposition is not mentioned. Daniel et al. [28] stated the importance of orienting the substrate perpendicular to the advancing barrier in order to achieve a more uniform monolayer deposition, while scanning tunnelling microscopy of phospholipid layers deposited on pyrolytic graphite revealed a uniform monolayer structure when the support was placed parallel to the moving barrier [29]. In this work, we studied the dependence of the transfer mode on the structure of the Cd arachidate (CdA) layers.

2. Experimental procedures

2.1. Spreading and deposition of vesicles

Vesicle suspensions of synthetic L- α -dimyristoylphosphatidylcholine (DMPC) in 50 mM sodium phosphate buffer at pH 6.0 were prepared by sonication. DMPC was obtained from Sigma; purity 99%. Membrane-bound enzyme ALDH was solubilized from the cell homogenate of *Glucobacter oxydans* with Triton X-100 detergent and further purified chromatographically in the presence of Triton X-100 [31]. Varying amounts of purified ALDH solutions in 10 mM sodium acetate buffer (pH 5.0) containing approx. 0.1–0.5% Triton X-100 was mixed with the vesicle suspensions for 30 min at 277 K. Triton X-100 was removed with Bio-Beads SM-2 nonpolar adsorbent 20–50 mesh (Bio-Rad) treatment. The incorporation of ALDH was confirmed in a separate experiment by ultracentrifugation (data not shown). The suspensions were either used as freshly prepared or stored at 253 K until used, to avoid denaturation of the protein. In some cases the suspensions were stored several months and we refer to these suspensions as aged vesicles. A KSV 2200 LB-balance was used for monolayer formation and deposition in a clean room under class 10 conditions. The vesicle suspensions were spread on a subphase containing 1 mM sodium acetate and 1 mM calcium chloride (pH of 5.8). The spreading was accomplished either dropwise directly onto the air/liquid interface or by running the suspension down a wet glass rod to the interface [32]. No difference in film formation was observed between the two spreading methods. The layers were transferred at a constant surface pressure of 25 mN/m with a deposition speed of 3 mm/min to clean glass slides or slides made hydrophobic with 9 layers of Cd arachidate. The horizontal lifting method was also used [33]. The transfer ratio for all deposited layers is shown in Table 1.

Table 1

The mean transfer ratios on the upward and downward movement of a glass slide on deposition of (a) 9 layers of cadmium arachidate (CdA) and transfer ratios for layers prepared from (b) aged and (c) freshly prepared vesicle suspensions

	Perpendicular		Parallel	
	on glass	on CdA	on glass	on CdA
(a)				
Up	0.88		0.89	
Down	0.90		0.95	
(b)			(c)	
Down	0.00	1.05	0.00	0.75
Up	0.75	0.04	0.50	0.05

The slide was positioned both perpendicular and parallel to the barrier.

2.2. Layers of Cd arachidate

Arachidic acid (Fluka, puriss) was dissolved at 1 mg/ml in chloroform (Aldrich, spectroscopic grade) and spread on a 0.3 mM cadmium chloride Millipore 'Milli-Q' water subphase (pH of 5.9). Glass slides were cleaned in chromic acid, rinsed in water and coated with 9 layers of Cd arachidate, CdA, at a surface pressure of 30 mN/m. The horizontal lifting and the conventional vertical deposition methods were used. A deposition speed of 3 mm/min was applied when depositing the slides vertically and the slides were positioned both perpendicular and parallel to the compressing barrier.

2.3. Atomic force microscopy

A Nanoscope II (Digital instruments, Santa Barbara, CA) AFM was used for the sample surface imaging. The scanner head D (15 μ m scan range) was applied with a 100 μ m cantilever of a spring constant k of 0.38 N/m [19]. The height mode was used to scan the surface; the distance and the force between the cantilever and the



Fig. 1. AFM image of a clean glass slide. In the nm colour scale bright corresponds to high and dark to low areas.

studied surface were kept constant by adjusting the z-piezo. All images (400×400 pixels) were measured in normal air conditions. The maximum attractive forces were typically in the range of 5–30 nN.

2.4. The quartz crystal microbalance

A quartz crystal was used to measure the amount of material deposited on its surface, as calculated from the deposition induced decrease in resonance frequency [34]. The employed QCM was a commercially available 10 MHz, AT-cut quartz crystal obtained from Universal Sensors, USA. The QCM was connected to a custom-made oscillator and driven at 5 V dc. The frequency of the vibrating quartz was measured by a universal frequency counter (HP 5316B).

3. Results and discussion

3.1. Layers of Cd arachidate

The topography of a clean glass slide and slides coated with 9 layers of CdA is shown in Figs. 1 and 2. Compared with the pure glass slide the vertically deposited CdA layers decrease the surface roughness at a nm-scale, but holes of various sizes are visible in the film. The holes appear dark in the images. The number and depth of these holes depend on how the slide was positioned in relation to the compressing barrier. Height profiles revealed that the depth of the holes was either 7 nm or 14 nm (± 0.5 nm), if the slide was positioned perpendicular to the barrier (Fig. 2a). This corresponds quite well to a bilayer or twice a bilayer thickness, assuming a monolayer thickness of 2.8 nm and an additive factor arising from the substrate roughness. The multilayer structure was much more homogeneous if the slide was positioned parallel to the compressing barrier during monolayer transfer (Fig. 2b). The number of holes was much less and their depth was about 6.6 nm, which agrees with the bilayer thickness. This implies that multilayers of CdA take up a head-to-head structure with holes of bilayer thickness or even twice a bilayer depending on transfer mode.

Horizontal deposition of CdA onto the QCM gave a linear decrease in frequency, with increasing number of layers indicating a homogeneous multilayer deposition. AFM images, however, revealed a non-uniform transfer of the film (Fig. 2c). The layers were often so fragmented that the μm -roughness even exceeded that of pure glass slides. However, the grain boundaries were well defined, i.e., the depths of the cracks and holes were an integer multiple, most often twice the monolayer thickness. Monolayer films of barium arachidate have been found to possess small holes when deposited by the horizontal deposition method [35]. Continuous horizontal deposition should give an X-type multilayer film structure, with the hy-

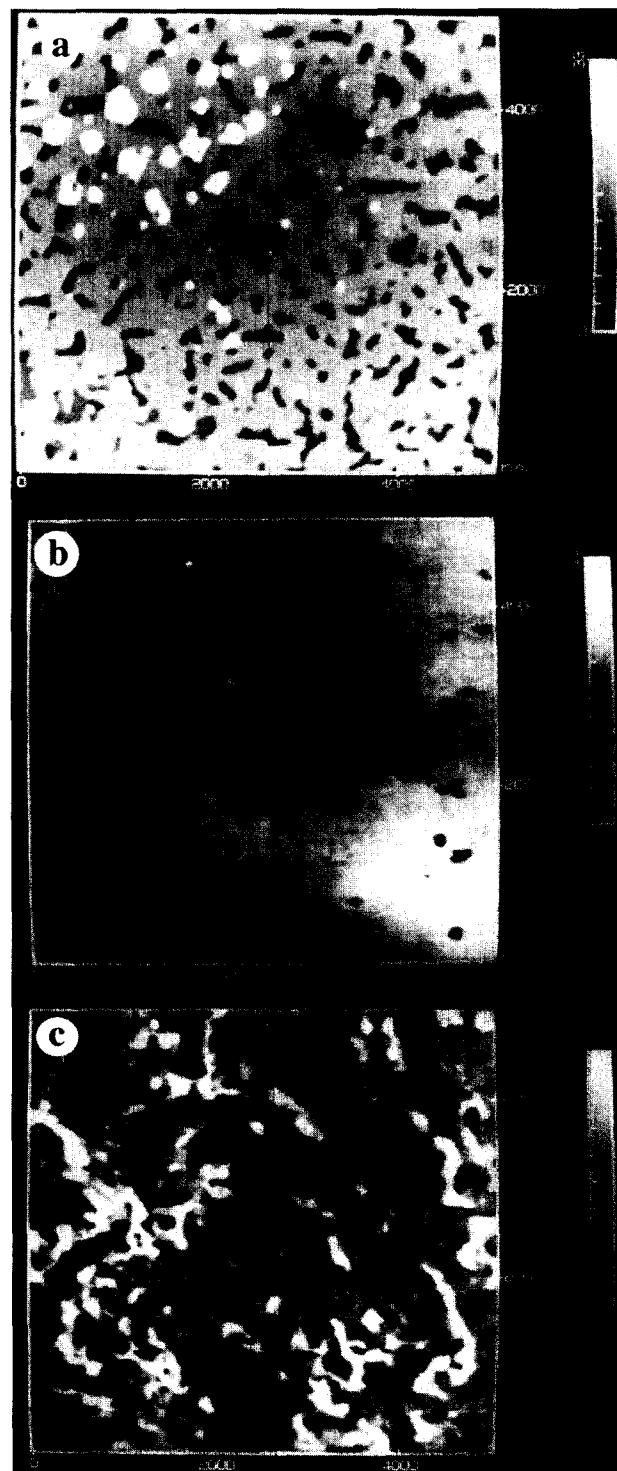


Fig. 2. AFM images of slides vertically coated with 9 layers of CdA with the slide positioned (a, top) perpendicular and (b, middle) parallel to the moving barrier and (c, bottom) by horizontal deposition. The height scales are in nm.

drophilic head groups of the molecules pointing out of the surface within each layer. This, however, seems unlikely for fatty acids. It has been postulated that multilayers of fatty acids have a Y-type structure irrespective of whether they are deposited in an X or Y-type sequence, so that

simple molecules like fatty acids are able to invert at some stage of the dipping process [27]. The observed non-uniform images could be due to a reorientation of the molecules – they overturn into a more favourable orientation. Reorganization has recently been observed for monolayers of CdA on mica surfaces held in the aqueous subphase [36]. In our case, the horizontal deposition was made manually, which also may have caused some disordering of the film.

3.2. Film formation of aged vesicles

When spreading an aged vesicle suspension onto the air/liquid interface the resulting layer had a characteristic compression isotherm similar in shape to that of pure DMPC spread from chloroform solutions. The mean molecular area of DMPC spread from pure lipid suspen-

sions was, however, only about 10% of that of DMPC spread from the chloroform solution. This indicates that most of the vesicles are not incorporated into the layer, but dissolve into the subphase or that most of the vesicles do not open. The isotherm was very stable with only minor changes in molecular area at constant surface pressure or on successive compression and expansion.

Films spread from both pure and various amounts of ALDH containing vesicles were transferred to glass slides. Fig. 3a shows the AFM image of a film from pure DMPC vesicles deposited horizontally onto a hydrophilic glass slide. Round objects of high density with an average height of 10–20 nm were visible on the slides. The diameter of the domains varied between 60–140 nm. This dimension was most probably affected by the convolution effects between the imaging tip and the domains. It was difficult to estimate the real diameter of the observed objects since the radius of curvature of the rounded tip was not exactly known and varies from one tip to another. Normally, the tip can be assumed to be round with a radius of about 50 nm, which according to a theoretical model presented by Butt et al. [37], gives a diameter of 10–50 nm for the objects. Horizontal deposition of films spread from DMPC/ALDH vesicle suspensions (image not shown) showed domains with a diameter of 300–600 nm. This would correspond to a real object diameter of about 110–450 nm. Thus the ALDH containing domains were clearly bigger than those observed from DMPC films.

If a vertical deposition was used the size of the domains was the same as for the horizontal deposition. The density was, however, much less as demonstrated in the image of a layer spread from DMPC/ALDH vesicle suspensions (Fig. 3b). A similar topography of the pure DMPC layer was obtained (image not shown), except for the smaller size of the domains. In some cases the vesicles deposited on glass formed queue-like clustering structures that predominantly appeared vertically aligned in the AFM image, i.e., perpendicular to the scanning direction. This may either be due to the vertical film transfer process or due to a reorganization of the layer structure during imaging. In fact, AFM has been used to move monolayer molecules laterally by adjusting the imaging force [18,22]. A perhaps less likely explanation would be localized regions of different frictional behaviour. The dynamical effect of an AFM tip on a monolayer has been studied by computer simulation of an atomic model [38]. However, this remained unchecked since the microscope used was not equipped with a friction measurement option.

The results suggest that the aged vesicles do not fuse to form a monolayer on the liquid interface, but are transferred as flattened aggregates to the solid slides. Large features of nonfused vesicles has also been obtained by Fare et al. [15]. Long-term storage at 277 K as well as freeze-thaw cycles enhances aggregation [39,40]. It seems obvious that the vesicles aggregate during storage at 253 K. Scanning tunneling microscope images showed a differ-

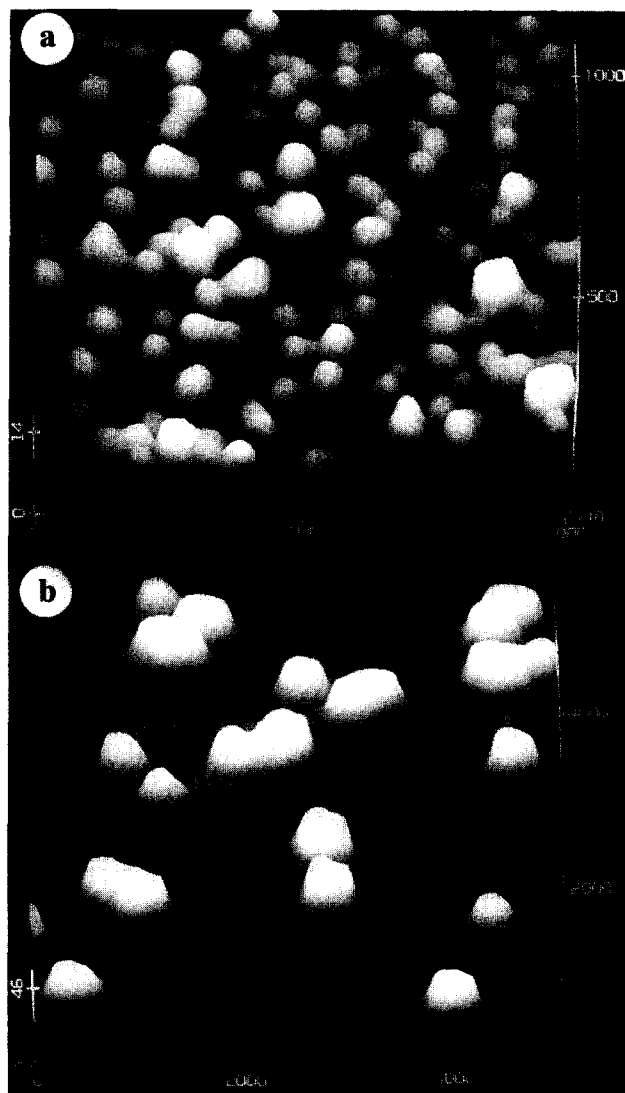


Fig. 3. AFM images of films transferred onto clean glass slides from (a, top) DMPC vesicles by horizontal and (b, bottom) DMPC/ALDH vesicles by vertical deposition.

ence in size for freshly prepared and aged vesicles. Our interpretation is that aged vesicles do not fuse because they are aggregated and that ALDH increased the size of these aggregates. Large nonfused vesicles have also been found to adhere to mica and glass when spread directly onto the surface from aged suspensions [20].

3.3. Film formation of fresh vesicles

Ultrasonic agitation is the most widely used method for converting lipid dispersions into single compartment vesicles of small size [41]. A different film formation was observed for vesicles spread from freshly prepared suspensions or when the vesicles were sonicated prior to spreading. The amount of material needed for film formation was much larger, but the isotherm characteristics were the same as for aged vesicles. The vertical deposition onto glass

slides previously coated with 9 layers of CdA was poor and the slide emerged wet on the upward movement, indicating that an inhomogeneous monolayer was transferred. The slide was positioned parallel to the compressing barrier and only one deposition cycle was carried out. The horizontal deposition onto hydrophobic slides was successful, whereas nothing stuck to hydrophilic slides, which emerged completely wet. Only one layer was deposited when using the horizontal dipping method. Fig. 4a and b shows AFM images of DMPC/ALDH films horizontally and vertically deposited on hydrophobic slides. Holes of various sizes could be observed on the images. The histograms show that most of the holes have a depth corresponding to a lipid monolayer with a thickness of about 3 nm. These holes are in agreement with the poor transfer ratio. A small amount of holes corresponding to a bilayer thickness could also be imaged. These are probably

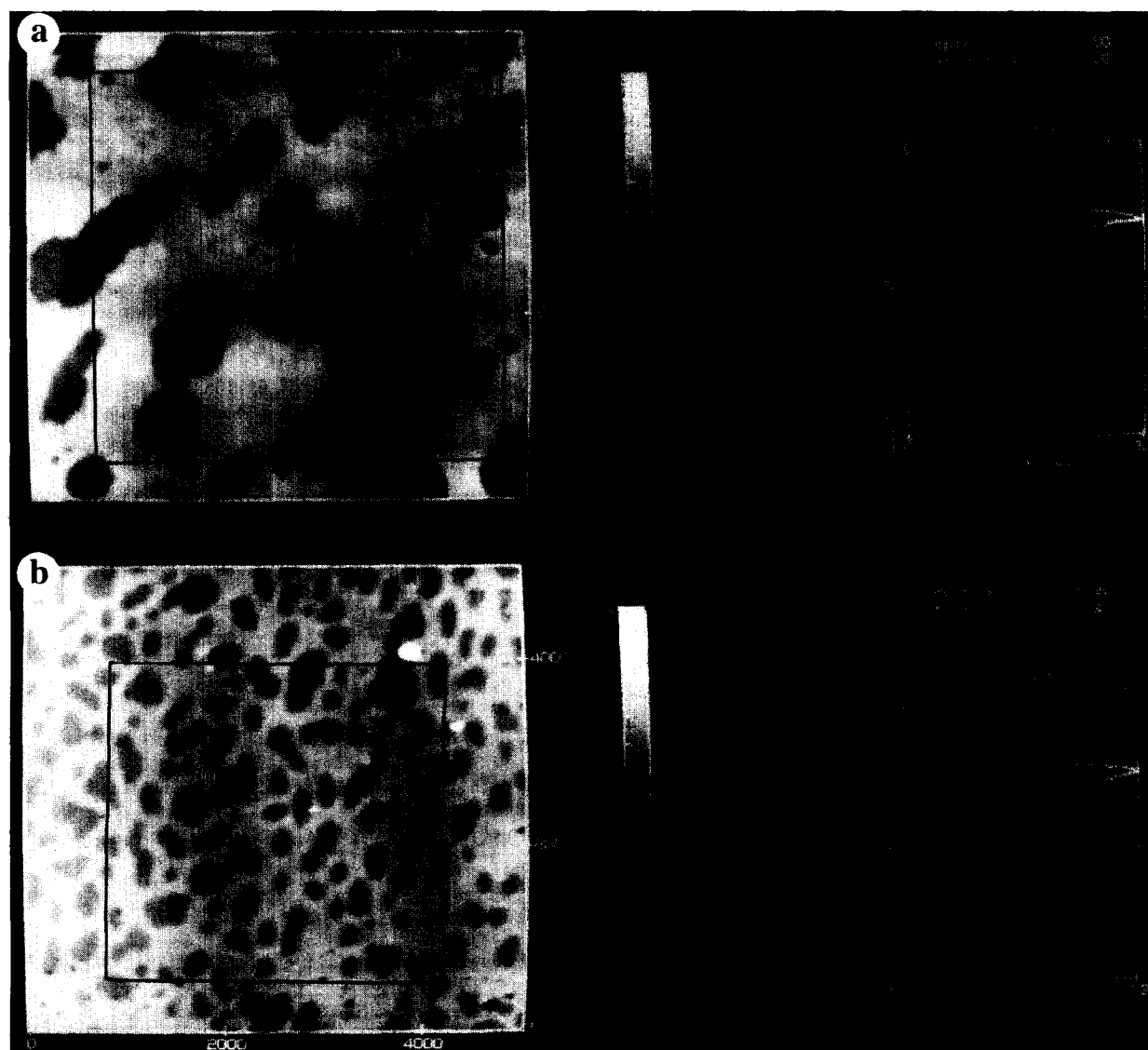


Fig. 4. AFM images of DMPC/ALDH spread from sonicated vesicles deposited by the (a, top) horizontal and (b, bottom) vertical dipping method on 9 layers of CdA. The height scales are in nm. The histograms to the right show depth in the enclosed area.

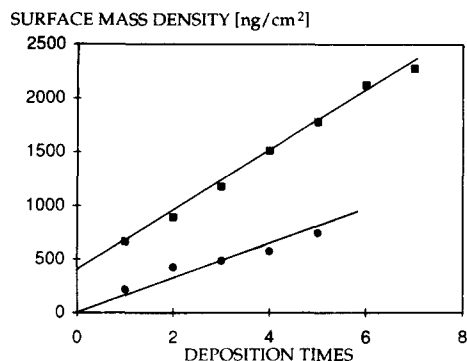


Fig. 5. Deposition onto a 10 MHz QCM of vesicles spread from an aged DMPC/ALDH suspension (■) and a freshly prepared DMPC suspension (●).

due to the underlying CdA layer and the holes therein. No domains could be imaged on the hydrophilic slides, which confirms that the film formation mechanism was different from that of aged vesicles. Our interpretation is that freshly prepared vesicles fuse at the air/liquid interface and can be transferred as a monolayer onto hydrophobic slides. Individual protein molecules are not immediately identifiable in the images, possible because of insufficient incorporation into the layers.

3.4. Quartz crystal deposition

Layers spread from aged DMPC/ALDH vesicles and from DMPC vesicles sonicated prior to spreading was transferred onto a 10 MHz quartz crystal by horizontal deposition (Fig. 5). The surface mass density increased linearly with the number of deposition cycles. A considerably larger amount of DMPC/ALDH was deposited on the first lifting of the crystal (670 ng/cm^2), compared to the following deposition sequences, which gave a linear increase in surface density of 330 ng/cm^2 . A much smaller increase in surface density of 190 ng/cm^2 was observed, when the crystal was coated with layers made up from sonicated DMPC vesicles. The mean molecular area of DMPC is about $0.52 \text{ nm}^2/\text{molecule}$, when spread from chloroform solutions [42]. This would give a surface density of 220 ng/cm^2 per layer. These results thus agree with our AFM data. Aged vesicles do not open – an amount more than a monolayer was deposited on the quartz crystal, but freshly prepared vesicles can be transferred as monolayers with a transfer ratio of 0.86. A lower transfer ratio of 0.75 was obtained on the upward movement for vertical deposition onto hydrophobic slides (Table 1). This is in agreement with the number of holes observed on the AFM images.

4. Conclusion

Care should be taken to obtain perfect layers when LB-films are to be used as supports for lipid films. The

order and topography of Cd arachidate multilayers depend on the transfer mode used. The slide should be placed parallel to the compressing barrier to obtain a homogeneous layer. Vesicles spread from aged suspensions do not open at the air/liquid interface, but are transferred as flattened structures. Unilamellar, freshly prepared or sonicated vesicles can be transferred as monolayers to the hydrophobic supports as imaged by atomic force microscopy. Enzyme molecules could, however, not be imaged because of the low enzyme concentration. In further work we will increase the concentration of enzymes in the film and determine the protein activity of the transferred films.

Acknowledgements

We thank M. Smolander at Biotechnology and Food Research, Technical Research Centre of Finland for preparing the vesicles.

References

- [1] Goldstein, L. and Manecke, G. (1976) in *Applied Biochemistry and Bioengineering* (Wingard, L.B., Katchalski-Katzir, Jr., E. and Goldstein, L., eds.), Vol. 1, pp. 23–125, Academic Press, New York.
- [2] Kochev, V. and Filljov, K. (1992) *Sensors Actuators* 8, 73–78.
- [3] Brian, A. and McConnel, H. (1984) *Proc. Natl. Acad. Sci. USA* 81, 6159–6163.
- [4] McConnel, H.M., Watts, T.H., Weis, R.M. and Brian, A.A. (1986) *Biochim. Biophys. Acta* 864, 95–106.
- [5] Steltze, M., Weissmüller, G. and Sackman, E. (1993) *J. Phys. Chem.* 97, 2974–2981.
- [6] Kalb, E. and Tamm, L.K. (1992) *Thin Solid Films* 210/211, 763–765.
- [7] Kalb, E., Frey, S. and Tamm L.K. (1992) *Biochim. Biophys. Acta* 1103, 307–316.
- [8] Xia, Z. and Van de Ven, T.G.M. (1992) *Langmuir* 8, 2938–2946.
- [9] Rädler, J. (1992) *Langmuir* 8, 848–853.
- [10] Ostro, M.J. (1987) *Sci. Am.* 256, 90–99.
- [11] Pattus, F., Desnuelle, P. and Verger, R. (1978) *Biochim. Biophys. Acta* 507, 62–70.
- [12] Pattus, F., Piovant, M.C.L., Lazdunski, C.J., Desnuelle, P. and Verger, R. (1978) *Biochim. Biophys. Acta* 507, 71–82.
- [13] Heyn, S.P., Egger, M. and Gaub, H.E. (1990) *J. Phys. Chem.* 94, 5073–5078.
- [14] Fischer, B., Heyn, S.P., Egger, M. and Gaub, H.E. (1993) *Langmuir* 9, 136–140.
- [15] Fare, T.L., Palmer, C.A., Silvestre, C.G., Cribbs, D.H., Turner, D.C., Brandow, S.L. and Gaber, B.P. (1992) *Langmuir* 8, 3116–3121.
- [16] Smolander, M., Livio, H.-L. and Räsänen, L. (1992) *Biosensors Bioelectronics* 7, 637–643.
- [17] Fujiwara, I., Ohnishi, M. and Seto, J. (1992) *Langmuir* 8, 2219–2222.
- [18] Lea, A., Pungor, S.A., Hlady, V., Andrade, J.D., Herron, J.N. and Voss, E.W. (1992) *Langmuir* 8, 68–73.
- [19] Peltonen, J., He, P. and Rosenholm, J. (1992) *J. Am. Chem. Soc.* 114, 7637–7642.
- [20] Singh, S. and Keller, D.J. (1991) *Biophys. J.* 60, 1401–1410.

- [21] Weisenhorn, A.L., Egger, M., Ohnesorge, F., Gould, S.A.C., Heyn, S.P., Hansma, H.G., Sinsheimer, R.L., Gaub, H.E. and Hansma, P.K. (1991) *Langmuir* 7, 8–12.
- [22] Weisenhorn, A.L., Drake, B., Prater, C.B., Gould, S.A.C., Hansma, P.K., Ohnesorge, F., Egger, M., Heyn, S.-P. and Gaub, H.E. (1990) *Biophys. J.* 58, 1251–1258.
- [23] Binks, B.P. (1991) *Adv. Colloid Interf. Sci.* 34, 343–432.
- [24] Viswanathan, R., Schwartz, D.K., Garnaes, J. and Zasadzinski, A.N. (1992) *Langmuir* 8, 1603–1607.
- [25] Morelis, R.M., Girard-Egrot, A.P. and Coulet, P.R. (1993) *Langmuir* 9, 3101–3106.
- [26] Girard-Egrot, A.P., Morelis, R.M. and Coulet, P.R. (1993) *Langmuir* 9, 3107–3110.
- [27] Petty, M.C. and Barlow, W.A. (1990) in *Langmuir Blodgett films* (Roberts, G., ed.), pp. 93–132, Plenum Press, New York.
- [28] Daniel, M.F. and Hart, J.T.T. (1985) *J. Mol. Electron.* 1, 97–104.
- [29] Niemi, H.E.-M., Ikonen, M., Levlin, J.M. and Lemmetyinen, H. (1993) *Langmuir* 9, 2436–2447.
- [30] Chi, L-F., Eng, L.M., Graf, K. and Fuchs, H. (1992) *Langmuir* 8, 2255–2261.
- [31] Smolander, M., Buchert, J. and Viikari, L. (1993) *J. Biotech.* 29, 287–297.
- [32] MacRitchie, F. (1986) *Adv. Colloid Interf. Sci.* 25, 341–385.
- [33] Nakahara, H. and Fukuda, K.J. (1979) *Colloid Interf. Sci.* 69, 24–33.
- [34] Sauerbrey, G.Z. (1959) *Z. Phys.* 155, 206–212.
- [35] Matsumoto, M., Uyeda, N., Fujiyosi, Y. and Aoyama, A. (1993) *Thin Solid Films* 223, 358–367.
- [36] Schwartz, D.K., Garnaes, J., Viswanathan, R. and Zasadzinski, J.A.N. (1992) *Science* 257, 508–511.
- [37] Butt, H-J. Guckenberger, R. and Rabe, J.P. (1992) *Ultramicroscopy* 46, 375–393.
- [38] Siepmann, I. (1993) *Tenside Surfactants Detergents* 30, 247– 251.
- [39] Coronado, R. and Labarca, P.P. (1984) *Trends Neurosci.* May, 155.
- [40] Yager, P. (1986) *Biosensors Bioelectronics* 2, 363–273.
- [41] New, R.R.C. (1990) in *Liposomes a practical approach* (New, R.R.C., ed.), pp. 33–103, Information Press, Oxford.
- [42] Marra, J. (1985) *J. Colloid Interf. Sci.* 107, 446–458.